19. K. D. Metzler, C. Goosmann, A. Lubojemska, A. Zychlinsky, V. Papayannopoulos, *Cell Rep.* **8**, 883–896 (2014).
20. J. S. Knight *et al.*, *Circ. Res.* **114**, 947–956 (2014).
21. R. T. Megens *et al.*, *Thromb. Haemost.* **107**, 597–598 (2012).
22. K. Kessenbrock *et al.*, *J. Clin. Invest.* **118**, 2438–2447 (2008).
23. A. Hakkim *et al.*, *Proc. Natl. Acad. Sci. U.S.A.* **107**, 9813–9818 (2010).
24. V. Papayannopoulos, D. Staab, A. Zychlinsky, *PLOS ONE* **6**, e28526 (2011).
25. H. Park *et al.*, *Nat. Immunol.* **6**, 1133–1141 (2005).
26. A. Walter *et al.*, *Nat. Commun.* **4**, 1560 (2013).
27. F. J. Sheedy *et al.*, *Nat. Immunol.* **14**, 812–820 (2013).
28. P. Bretscher *et al.*, *EMBO Mol. Med.* **7**, 593–607 (2015).
29. V. Hornung, E. Latz, *Nat. Rev. Immunol.* **10**, 123–130 (2010).
30. Y. Miyake, S. Yamasaki, *Adv. Exp. Med. Biol.* **738**, 144–152 (2012).
31. R. Lande *et al.*, *Nature* **449**, 564–569 (2007).
32. C. Koulis *et al.*, *Arterioscler. Thromb. Vasc. Biol.* **34**, 516–525 (2014).
33. S. Horibata, S. A. Coonrod, B. D. Cherrington, *J. Reprod. Dev.* **58**, 274–282 (2012).
34. P. Goossens *et al.*, *Cell Metab.* **12**, 142–153 (2010).
35. V. A. Rathinam *et al.*, *Cell* **150**, 606–619 (2012).
36. P. Broz *et al.*, *Nature* **490**, 288–291 (2012).
37. R. Khandpur *et al.*, *Sci. Transl. Med.* **5**, 178ra40 (2013).
38. K. D. Metzler *et al.*, *Blood* **117**, 953–959 (2011).

ACKNOWLEDGMENTS

We thank Q. Xu for providing the *ApoE*$^{-/-}$ mice and A. Zychlinsky for the *PR3/NE*$^{-/-}$ mice; Z. Zhang for training; L. Mrowietz for help with NET preparations; and B. Stockinger, A. Zychlinsky, A. Schaefer, and M. Wilson for comments on the manuscript. This work was supported by the UK Medical Research Council (grant MC_UP_1202/13) and was principally conducted at the MRC National Institute for Medical Research and completed at the Francis Crick Institute, which receives its core funding from the UK Medical Research Council, Cancer Research UK, and the Wellcome Trust. The data are contained in the manuscript and the supplementary materials.

SUPPLEMENTARY MATERIALS

www.sciencemag.org/content/349/6245/316/suppl/DC1
Materials and Methods
Supplementary Text
Figs. S1 to S13
References (*39*, *40*)

30 January 2015; accepted 8 June 2015
10.1126/science.aaa8064

HIV-1 VACCINES

Protective efficacy of adenovirus/protein vaccines against SIV challenges in rhesus monkeys

Dan H. Barouch,[1,2]* Galit Alter,[2] Thomas Broge,[2] Caitlyn Linde,[2] Margaret E. Ackerman,[3] Eric P. Brown,[3] Erica N. Borducchi,[1] Kaitlin M. Smith,[1] Joseph P. Nkolola,[1] Jinyan Liu,[1] Jennifer Shields,[1] Lily Parenteau,[1] James B. Whitney,[1] Peter Abbink,[1] David M. Ng'ang'a,[1] Michael S. Seaman,[1] Christy L. Lavine,[1] James R. Perry,[1] Wenjun Li,[4] Arnaud D. Colantonio,[5] Mark G. Lewis,[6] Bing Chen,[7] Holger Wenschuh,[8] Ulf Reimer,[8] Michael Piatak,[9]† Jeffrey D. Lifson,[9] Scott A. Handley,[10] Herbert W. Virgin,[10] Marguerite Koutsoukos,[11] Clarisse Lorin,[11] Gerald Voss,[11] Mo Weijtens,[12] Maria G. Pau,[12] Hanneke Schuitemaker[12]

Preclinical studies of viral vector–based HIV-1 vaccine candidates have previously shown partial protection against neutralization-resistant virus challenges in rhesus monkeys. In this study, we evaluated the protective efficacy of adenovirus serotype 26 (Ad26) vector priming followed by purified envelope (Env) glycoprotein boosting. Rhesus monkeys primed with Ad26 vectors expressing SIVsmE543 Env, Gag, and Pol and boosted with AS01B-adjuvanted SIVmac32H Env gp140 demonstrated complete protection in 50% of vaccinated animals against a series of repeated, heterologous, intrarectal SIVmac251 challenges that infected all controls. Protective efficacy correlated with the functionality of Env-specific antibody responses. Comparable protection was also observed with a similar Ad/Env vaccine against repeated, heterologous, intrarectal SHIV-SF162P3 challenges. These data demonstrate robust protection by Ad/Env vaccines against acquisition of neutralization-resistant virus challenges in rhesus monkeys.

Despite the urgent need for a safe and effective global HIV-1 vaccine, only four vaccine concepts have been evaluated for protective efficacy in humans during more than 30 years (*1*, *2*). In rhesus monkeys, vaccine protection has been reported against neutralization-sensitive viruses (*3*), but these data failed to predict protective efficacy in humans (*4*), which suggests the importance of using neutralization-resistant virus challenges for preclinical evaluation of HIV-1 and SIV vaccine candidates. We previously showed that priming with adenovirus vectors and boosting with poxvirus vectors expressing Env, Gag, and Pol resulted in a reduced per-exposure acquisition risk after challenges with neutralization-resistant SIVmac251, but the majority of these animals were infected at the end of the challenge series (*5*, *6*). To augment antibody responses, we evaluated the immunogenicity and protective efficacy of priming with adenovirus vectors and boosting with adjuvanted Env gp140 protein against SIVmac251 and SHIV-SF162P3 challenges in rhesus monkeys.

We immunized 32 adult rhesus monkeys (*Macaca mulatta*) that did not express the protective major histocompatibility complex class I alleles *Mamu-A*01*, *Mamu-B*08*, or *Mamu-B*17* with adenovirus serotype 26 (Ad26) vectors (*7*) expressing SIVsmE543 Env/Gag/Pol antigens (*5*) followed by either SIVmac32H Env gp140 protein (*8*) (Ad/Env; $n = 12$) or Ad35 vectors (*9*) expressing SIVsmE543 Env/Gag/Pol antigens (Ad Alone; $n = 12$), and a control group received sham vaccines (Sham; $n = 8$). Animals in the Ad/Env group were primed with 3×10^{10} viral particles (vp) Ad26-Env/Gag/Pol vectors (10^{10} vp per vector) by the intramuscular route at weeks 0 and 24 and were boosted with 0.25 mg Env gp140 with AS01B Adjuvant System at weeks 52, 56, and 60. Animals in the Ad Alone group were primed with 3×10^{10} vp Ad26-Env/Gag/Pol vectors at weeks 0 and 24 and were boosted with 3×10^{10} vp Ad35-Env/Gag/Pol at week 52. One control animal died before challenge for reasons unrelated to the study protocol and was excluded from the analysis.

Binding antibody responses to heterologous SIVmac239 Env gp140 were detected by enzyme-linked immunosorbent assay (ELISA) (*10*) in all vaccinated animals after Ad26 priming at weeks 4 and 28 (Fig. 1A). In the Ad/Env group, ELISA end-point titers increased from 5.3 logs at week 28 to 6.4 logs after the SIV Env gp140 boosts at week 64 ($P < 0.0001$) (Fig. 1A), which confirmed that the Env boost effectively augmented Ad26-primed antibody responses. Neutralizing antibody (NAb) responses assessed in the TZM-bl cell line (*11*) against tier 1 heterologous SIVmac251_TCLA.15 and homologous SIVsmE660 CP3C-P-A8 viruses also increased significantly after SIV Env gp140 boosting (fig. S1). NAb responses against tier 2 viruses were borderline (fig. S1).

In addition to neutralization, antibodies mediate a wide variety of additional antiviral functions through their ability to interact with Fc receptors, complement, and lectin-like proteins

[1]Center for Virology and Vaccine Research, Beth Israel Deaconess Medical Center, Harvard Medical School, Boston, MA 02215, USA. [2]Ragon Institute of Massachusetts General Hospital, Massachusetts Institute of Technology, and Harvard University, Cambridge, MA 02139, USA. [3]Thayer School of Engineering at Dartmouth, Hanover, NH 03755, USA. [4]University of Massachusetts Medical School, Worcester, MA 01605, USA. [5]New England Primate Research Center, Southborough, MA 01772, USA. [6]Bioqual, Rockville, MD 20852, USA. [7]Children's Hospital, Boston, MA 02115, USA. [8]JPT Peptide Technologies GmbH, 12489 Berlin, Germany. [9]AIDS and Cancer Virus Program, Leidos Biomedical Research, Frederick National Laboratory, Frederick, MD 21702, USA. [10]Washington University School of Medicine, St. Louis, MO 63110, USA. [11]GSK Vaccines, 1330 Rixensart, Belgium. [12]Janssen Infectious Diseases and Vaccines (formerly Crucell), 2301 Leiden, Netherlands
†Deceased. ***Corresponding author. E-mail: dbarouch@bidmc.harvard.edu**

(*12*, *13*). Previous studies showed that antibody-dependent cellular phagocytosis (ADCP) (*14*) and antibody-dependent complement deposition (ADCD) responses correlated with protective efficacy in rhesus monkeys (*6*). To perform a comprehensive analysis of vaccine-elicited antibody responses, we evaluated 150 independent antibody Fc parameters by high-throughput antibody profiling, including multiple assessments of antibody Fc functionality [ADCP, ADCD, antibody-dependent cell-mediated cytotoxicity (ADCC), antibody-dependent NK cell expression of CD107a, interferon-γ (IFN-γ), and the chemokine CCL4], isotypes, glycosylation, complement binding, and Fc receptor binding (*14*–*18*). Integration of all 3600 data points in a principal-component analysis demonstrated that the Ad/Env vaccine and the Ad Alone vaccine elicited Env-specific antibodies that were phenotypically distinct ($P < 0.0001$) (Fig. 1B). A loadings plot (Fig. 1C) showed the distribution of all measured Fc features in the same multidimensional space, which demonstrated the specific features that drove the separation of antibody profiles (red arrows). Partial least-squares discriminant analysis (*19*) revealed that the six antibody Fc functions described above nearly completely separated these groups, with the majority of antibody Fc effector functions clustering with the Ad/Env–vaccinated animals (Fig. 1D). Univariate analyses showed that these antibody Fc functions were all significantly increased in Ad/Env group as compared with the Ad Alone group (Fig. 1E), and a combined analysis demonstrated that the number of antibody Fc functions was significantly greater in Ad/Env-vaccinated animals as compared with animals vaccinated with Ad Alone (Fig. 1, F and G). These data show that the protein boost resulted in a more polyfunctional antibody Fc effector profile.

Cellular immune responses measured by IFN-γ enzyme-linked immunospot (ELISPOT) assays in response to heterologous SIVmac239 and homologous SIVsmE543 Env/Gag/Pol peptide pools were also detected in all animals after vaccination (fig. S2). By multiparameter intracellular cytokine staining assays, SIV Env gp140 boosting primarily expanded Env-specific IFN-γ^+CD4^+ T lymphocyte responses in the Ad/Env group, whereas Ad35-Env/Gag/Pol boosting substantially expanded IFN-γ^+CD8^+ T lymphocyte responses in the Ad Alone group (fig. S2). Both $CD28^+CD95^+$ central and transitional memory and $CD28^+CD95^-$ effector memory $CD4^+$ and $CD8^+$ T lymphocyte responses (*20*, *21*) were elicited by both vaccines (fig. S3).

To evaluate the protective efficacy of these vaccine regimens, all animals were challenged with six repeated, intrarectal inoculations with 500 tissue culture infectious doses ($TCID_{50}$) of the heterologous, neutralization-resistant virus SIVmac251 (*5*, *22*, *23*) beginning week 96 (Fig. 2, A and B). All control animals were infected by this challenge protocol. The Ad Alone vaccine regimen resulted in a 75% reduction in the per-exposure acquisition risk as compared with controls [1 – (hazard ratio); $P = 0.039$, Cox proportional hazard model], which is consistent with our prior studies (*5*). In contrast, the Ad/Env vaccine regimen afforded a 90% reduction in the per-exposure acquisition risk as compared with controls ($P = 0.001$). Moreover, 50% (6 of 12) of animals in this group also appeared uninfected at the end of this challenge protocol ($P = 0.012$ compared with controls, chi-square test; $P = 0.044$, Fisher's exact test) (Fig. 2B). Protection in the Ad/Env group was greater than that in the Ad Alone group ($P = 0.042$, chi-square test; $P = 0.097$, Fisher's exact test). Binding antibody titers [$P < 0.0001$; correlation coefficient (R) = 0.75] and antibody Fc polyfunctionality

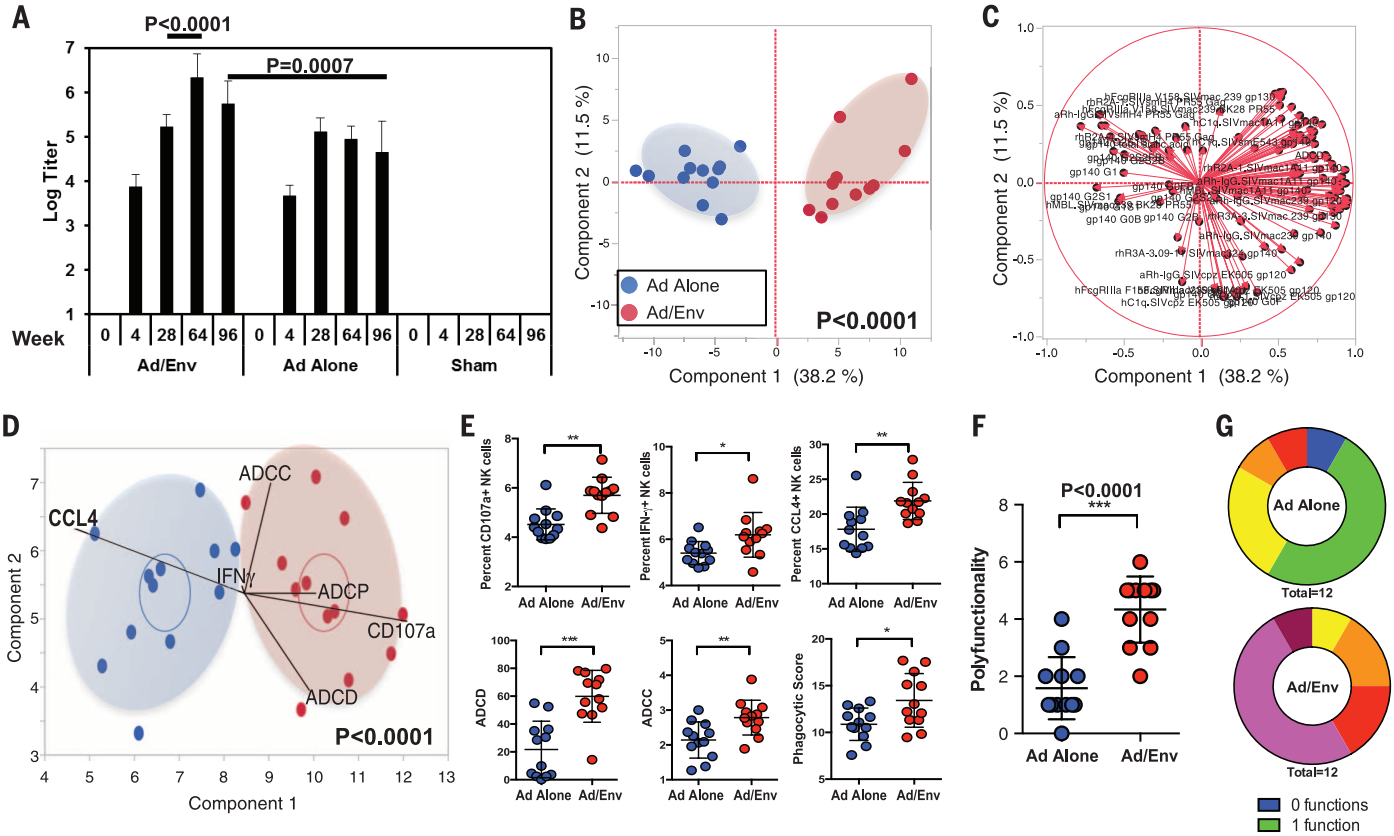

Fig. 1. Humoral immune responses elicited by the Ad26/Env SIV vaccine. (**A**) SIVmac239 Env-specific ELISA titers at weeks 0, 4, 28, 64, and 96. Mean log end-point ELISA titers are shown. (**B** to **G**) Multidimensional analysis integrating 150 antibody Fc parameters per animal demonstrates differences in antibody Fc profiles. (B) Principal component analysis (PCA) of antibody Fc profiles from animals immunized with Ad/Env (red) or Ad Alone (blue) vaccines. (C) Loadings plot mirrors the multidimensional space in the PCA but shows the distribution of all measured Fc features, which demonstrates the features that drove the separation of antibody profiles (red arrows). (D) Partial least-squares discriminant analysis (PLSDA) of antibody profiles from Ad/Env and Ad Alone vaccinees. (E) Univariate analyses of antibody functions identified in (D). A composite (F) dot plot and (G) pie chart show the overall functionality of antibody responses elicited by the Ad/Env and the Ad Alone vaccines. Error bars reflect SEM. *P* values reflect Mann-Whitney tests. *$P < 0.01$, **$P < 0.001$, ***$P < 0.0001$.

(P = 0.004; R = 0.56) best correlated with protection against acquisition of infection, as measured by the number of challenges required for infection (Fig. 2C). Individual antibody functions (ADCP, ADCC, CD107, CCL4) also correlated with protection (P < 0.05).

In the Ad/Env group, plasma viral loads were persistently negative in the six protected monkeys for 400 days after challenge (Fig. 2D). Of the six infected animals in this group, four animals developed measureable chronic set-point viremia, whereas two monkeys exhibited transient acute viremia and subsequently became elite controllers with undetectable plasma viral loads (Fig. 2D and fig. S4). In the Ad Alone group, plasma viral loads were persistently negative in 2 of 12 monkeys, and chronic viremia developed in 10 of 12 animals. In contrast, all sham controls developed high levels of chronic viremia with a median set-point viral load from days 100 to 400 after infection of 6.03 log copies/ml, which was at least 1.65 logs as high as the median set-point viral load in the animals in the Ad/Env group that became infected (P = 0.035) (fig. S5).

We previously reported that progressive SIV infection correlated with a marked expansion of the enteric virome in rhesus monkeys, particularly for picornavirus reads (*24*–*27*). Metagenomics sequencing of stool samples in the present study demonstrated that the enteric virome expanded by week 28 but not by week 10 in the sham controls (P = 0.015) (fig. S6). Both the Ad/Env and the Ad Alone vaccines reduced the expansion of total enteric reads including enteric picornaviruses (P = 0.002 and P = 0.042, respectively) (fig. S6). The Ad/Env vaccine also reduced AIDS-related mortality as compared with the sham controls (P = 0.020) (fig. S7).

We next investigated whether the vaccinated animals that exhibited persistently negative plasma viral loads were completely protected by comprehensive tissue analyses, adoptive transfer studies, and immunologic assays. We performed necropsies on the six protected animals in the Ad/Env group, the two protected animals in the Ad Aone group, and one of the elite controllers in the Ad/Env group at ~400 days after challenge (Fig. 2D). All of these animals had negative plasma viral loads at the time of necropsy. We assessed 36 gastrointestinal, lymphoid, and reproductive tract tissues per animal (28 tissues in males) by ultrasensitive nested quantitative polymerase chain reaction or quantitative reverse transcription polymerase chain reaction assays for SIV DNA and SIV RNA as previously described (*28*). Viral DNA and RNA were readily detectable in all tissues in the elite controller (Fig. 3A, red circles) but not in the eight protected animals (Fig. 3A, black circles), except for one viral signal in a single animal, which is within the range of expected background false-positive signals in similar analyses of naïve animals (*28*).

We next performed adoptive transfer studies and infused 60 million peripheral blood and lymph node mononuclear cells by the intravenous route from the eight apparently protected animals and the two elite controllers into naïve rhesus monkey hosts. Cells from the elite controllers readily transferred infection and resulted in plasma viral loads of 6.87 to 7.12 log copies/ml in naïve recipients by day 14 after adoptive transfer (Fig. 3B, red lines). In contrast, cells from the

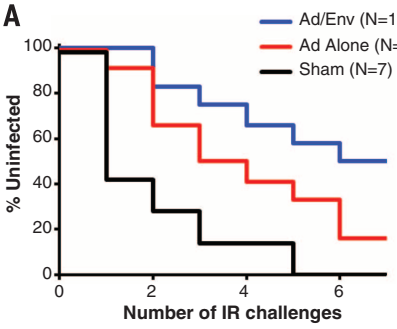

B

	Hazard Ratio (95% CI)	Per-Exposure Risk Reduction	P-Value vs Sham[1]	P-Value vs Sham[2]	Complete Protection	P-Value vs Sham[3]	P-Value vs Sham[4]
Ad/Env	0.095 (0.023-0.402)	90%	0.001	0.001	50%	0.012	0.044
Ad Alone	0.251 (0.068-0.933)	75%	0.039	0.048	17%	0.127	0.509
Sham	1 (reference)	N/A	N/A	N/A	0%	N/A	N/A
	[1]Cox proportional hazard model; [2]Log-rank test				[3]Chi-square test; [4]Fisher's exact test		

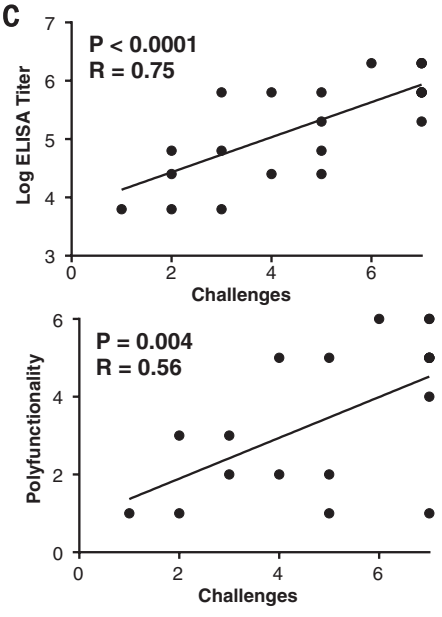

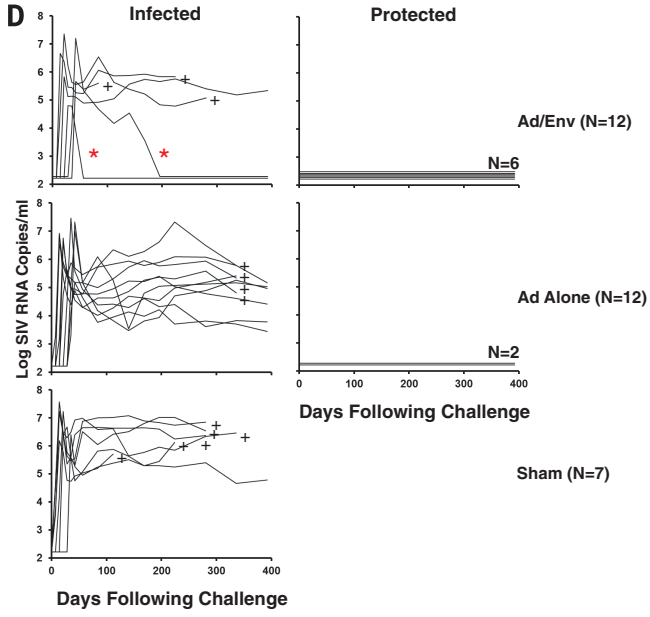

Fig. 2. Protective efficacy of the Ad26/Env SIV vaccine against repeated, intrarectal SIVmac251 challenges. (**A**) Number of challenges required for acquisition of infection in each vaccine group. (**B**) Statistical analyses include the hazard ratio with 95% confidence interval and the per-exposure reduction of acquisition risk in each group, with P values reflecting Cox proportional hazard models and log-rank tests. Additional statistical analyses include the percentage of completely protected animals at the end of the challenge series, with P values reflecting chi-square tests and Fisher's exact tests. (**C**) Correlation of log ELISA titers and antibody Fc polyfunctionality at week 64 with the number of challenges required to establish infection. The plotted data reflect only vaccinated animals and do not include the sham controls. Values plotted as >6 challenges reflect animals that remained uninfected. Overlapping data points are shown as a single symbol. P values reflect Spearman rank correlation tests. (**D**) Plasma SIV RNA copies/ml over time in infected and protected animals in each vaccine group. Red asterisks indicate elite controllers. + indicates mortality.

protected animals failed to transfer infection (Fig. 3B, black lines).

Furthermore, the protected animals exhibited no increase in Env/Gag/Pol-specific cellular immune responses after challenge and also no responses to Vif, which was not included in the vaccine, whereas vaccinated animals that became infected developed massive anamnestic Env/Gag/Pol-specific cellular immune responses and primary Vif-specific responses (fig. S8). The protected animals also exhibited no anamnestic Env-specific ELISA antibody responses after challenge. Taken together (Fig. 3 and fig. S8), these data strongly suggest that the Ad/Env vaccine afforded complete sterilizing protection in 50% of animals against the SIVmac251 challenge protocol and that the mechanism of protection involved primary blocking of acquisition of infection.

To confirm these findings with analogous vaccines expressing HIV-1 immunogens, we used a group of 20 rhesus monkeys that had been immunized previously at weeks 0 and 40 with Ad26 and Ad5HVR48 vectors expressing mosaic, consensus, or natural clade C HIV-1 Env/Gag/Pol immunogens (*29*). Two years after Ad priming, these animals were boosted six times with 0.25 mg HIV-1 clade C C97ZA012 Env gp140 (*10*, *30*) with the AS01B Adjuvant System at weeks 156, 160, 164, 176, 180, and 184 (Ad/Env; n = 20). A second group of animals received only 0.25 mg Env gp140 with AS01B at the same six time points (Env Alone; n = 8), and a third control group received sham vaccines (Sham; n = 12). The Ad/Env vaccine elicited greater antibody responses than did the Env Alone vaccine by ELISA (fig. S9); functional nonneutralizing antibody assays (*6*, *14*, *15*) (fig. S9); tier 1 NAb TZM-bl assays (fig. S10); tier 2 NAb A3R5 assays (fig. S11); and linear peptide microarray assays (*31*, *32*), including variable region 2–specific responses (*33*, *34*) (fig. S12). Protective efficacy was assessed by six intrarectal challenges with 500 $TCID_{50}$ of the heterologous, neutralization-resistant virus SHIV-SF162P3 (*6*) beginning week 196 (Fig. 4, A and B). Although the Env Alone vaccine afforded only minimal protection, 40% (8 of 20) of Ad/Env-vaccinated animals were completely protected against this challenge series (P = 0.006 compared with controls, chi-square test; P = 0.014, Fisher's exact test) (Fig. 4B and figs. S13 to S15). Binding antibody titers (P = 0.008) and ADCP responses (P = 0.001) correlated with protection against acquisition of infection.

Our data demonstrate the protective efficacy of Ad/Env vaccine regimens against SIVmac251 and SHIV-SF162P3 challenges in rhesus monkeys and suggest that the Env protein boost improved protective efficacy by enhancing the functionality of vaccine-elicited, Env-specific antibody responses. In contrast, DNA/Ad5 vaccines afforded

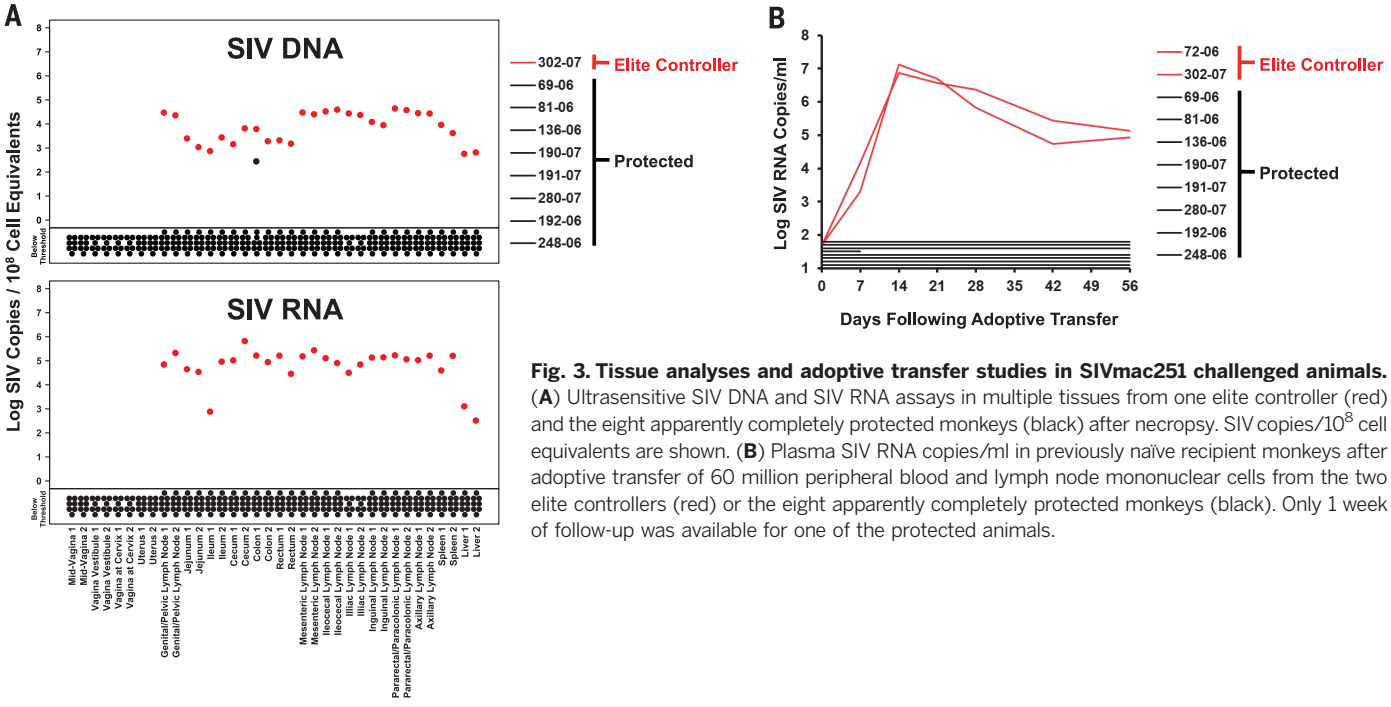

Fig. 3. Tissue analyses and adoptive transfer studies in SIVmac251 challenged animals. (**A**) Ultrasensitive SIV DNA and SIV RNA assays in multiple tissues from one elite controller (red) and the eight apparently completely protected monkeys (black) after necropsy. SIV copies/10^8 cell equivalents are shown. (**B**) Plasma SIV RNA copies/ml in previously naïve recipient monkeys after adoptive transfer of 60 million peripheral blood and lymph node mononuclear cells from the two elite controllers (red) or the eight apparently completely protected monkeys (black). Only 1 week of follow-up was available for one of the protected animals.

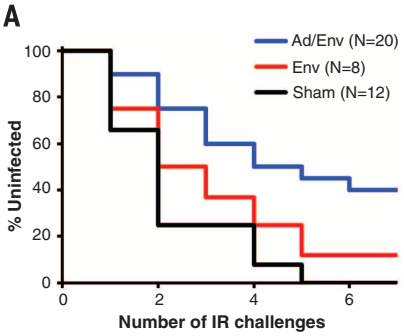

B

	Hazard Ratio (95% CI)	Per-Exposure Risk Reduction	P-Value vs Sham[1]	P-Value vs Sham[2]	Complete Protection	P-Value vs Sham[3]	P-Value vs Sham[4]
Ad/Env	0.212 (0.078-0.581)	79%	0.003	0.002	40%	0.006	0.014
Env	0.513 (0.161-1.636)	49%	0.259	0.289	12%	0.104	0.400
Sham	1	N/A	N/A	N/A	0%	N/A	N/A
	[1]Cox proportional hazard model; [2]Log-rank test				[3]Chi-square test; [4]Fisher's exact test		

Fig. 4. Protective efficacy of the Ad/Env HIV-1 vaccine against repeated, intrarectal SHIV-SF162P3 challenges. (**A**) Number of challenges required for acquisition of infection in each vaccine group. (**B**) Statistical analyses include the hazard ratio with 95% confidence interval and the per exposure reduction of acquisition risk in each group, with P values reflecting Cox proportional hazard models and log-rank tests. Additional statistical analyses include the percentage of completely protected animals at the end of the challenge series, with P values reflecting chi-square tests and Fisher's exact tests.

no protection against SIVmac251 challenges (*3*), which reflects the ability of DNA/Ad5 vaccines to block only neutralization-sensitive virus clones (*35*). Alphavirus vector priming and Env protein boosting afforded partial protection against the neutralization-sensitive virus SHIV-SF162P4 but was not evaluated against neutralization-resistant viruses (*36*). Rhesus cytomegalovirus (CMV) vectors failed to block acquisition of infection but afforded post-infection virologic control and eventual viral clearance in about half of the animals after SIVmac239 challenges (*28*, *37*).

The protective efficacy of Ad/Env vaccines against acquisition of neutralization-resistant virus challenges in rhesus monkeys in the present study has important implications for HIV-1 vaccine development and suggests the potential of Env protein boosting after Ad vector priming. Nevertheless, important differences exist between SIV/SHIV infection in rhesus monkeys and HIV-1 infection in humans. Clinical efficacy studies are therefore required to determine the protective efficacy of these HIV-1 vaccine candidates in humans.

REFERENCES AND NOTES

1. A. S. Fauci, H. D. Marston, *N. Engl. J. Med.* **370**, 495–498 (2014).
2. D. H. Barouch, *N. Engl. J. Med.* **369**, 2073–2076 (2013).
3. N. L. Letvin *et al.*, *Sci. Transl. Med.* **3**, 81ra36 (2011).
4. S. M. Hammer *et al.*, *N. Engl. J. Med.* **369**, 2083–2092 (2013).
5. D. H. Barouch *et al.*, *Nature* **482**, 89–93 (2012).
6. D. H. Barouch *et al.*, *Cell* **155**, 531–539 (2013).
7. P. Abbink *et al.*, *J. Virol.* **81**, 4654–4663 (2007).
8. B. Chen *et al.*, *J. Biol. Chem.* **275**, 34946–34953 (2000).
9. R. Vogels *et al.*, *J. Virol.* **77**, 8263–8271 (2003).
10. J. P. Nkolola *et al.*, *J. Virol.* **84**, 3270–3279 (2010).
11. D. Montefiori, *Curr. Protoc. Immunol.* **Chap. 12** (Unit 12.11), 1–15 (2005).
12. A. W. Chung, G. Alter, *Future Virol* **9**, 397–414 (2014).
13. M. E. Ackerman, G. Alter, *Curr. HIV Res.* **11**, 365–377 (2013).
14. M. E. Ackerman *et al.*, *J. Immunol. Methods* **366**, 8–19 (2011).
15. V. R. Gómez-Román *et al.*, *J. Immunol. Methods* **308**, 53–67 (2006).
16. A. W. Chung *et al.*, *Sci. Transl. Med.* **6**, 228ra38 (2014).
17. E. P. Brown *et al.*, *J. Immunol. Methods* **386**, 117–123 (2012).
18. A. W. Boesch *et al.*, *MAbs* **6**, 915–927 (2014).
19. K. S. Lau *et al.*, *Sci. Signal.* **4**, ra16 (2011).
20. L. J. Picker *et al.*, *J. Clin. Invest.* **116**, 1514–1524 (2006).
21. H. Li *et al.*, *J. Virol.* **85**, 11007–11015 (2011).
22. J. Liu *et al.*, *Nature* **457**, 87–91 (2009).
23. J. Liu *et al.*, *J. Virol.* **84**, 10406–10412 (2010).
24. S. A. Handley *et al.*, *Cell* **151**, 253–266 (2012).
25. E. Aronesty, in code.google.com/p/ea-utils. (ea-utils, Durham, NC, 2011).
26. L. Fu, B. Niu, Z. Zhu, S. Wu, W. Li, *Bioinformatics* **28**, 3150–3152 (2012).
27. D. H. Huson, S. Mitra, H.-J. Ruscheweyh, N. Weber, S. C. Schuster, *Genome Res.* **21**, 1552–1560 (2011).
28. S. G. Hansen *et al.*, *Nature* **502**, 100–104 (2013).
29. D. H. Barouch *et al.*, *Nat. Med.* **16**, 319–323 (2010).
30. J. M. Kovacs *et al.*, *Proc. Natl. Acad. Sci. U.S.A.* **109**, 12111–12116 (2012).
31. A. Masch, J. Zerweck, U. Reimer, H. Wenschuh, M. Schutkowski, *Methods Mol. Biol.* **669**, 161–172 (2010).
32. K. E. Stephenson *et al.*, *J. Immunol. Methods* **416**, 105–123 (2015).
33. S. Rerks-Ngarm *et al.*, *N. Engl. J. Med.* **361**, 2209–2220 (2009).
34. B. F. Haynes *et al.*, *N. Engl. J. Med.* **366**, 1275–1286 (2012).
35. M. Roederer *et al.*, *Nature* **505**, 502–508 (2014).
36. S. W. Barnett *et al.*, *J. Virol.* **84**, 5975–5985 (2010).
37. S. G. Hansen *et al.*, *Nature* **473**, 523–527 (2011).

ACKNOWLEDGMENTS

We thank M. Pensiero, M. Marovich, M. Beck, J. Kramer, S. Westmoreland, P. Johnson, W. Wagner, J. Yalley, C. Gittens, C. Cosgrove, M. Kumar, J. Schmitz, H. Peng, J. Hendriks, D. van Manen, W. Bosche, V. Cyril, Y. Li, F. Stephens, R. Hamel, K. Kelly, and L. Dunne for generous advice, assistance, and reagents. The SIVmac239 peptides were obtained from the NIH AIDS Research and Reference Reagent Program. The data presented in this paper are tabulated in the main paper and in the supplementary materials. The authors declare no competing financial interests. D.H.B. is a named co-inventor on vector, antigen, and protein patents (PCT/EP2007/052463, PCT/US2009/060494, PCT/US2009/064999). Correspondence and requests for materials should be addressed to D.H.B. (dbarouch@bidmc.harvard.edu). Vectors, antigens, proteins, adjuvants, and viruses are subject to Material Transfer Agreements. We acknowledge support from the NIH (AI060354, AI078526, AI080289, AI084794, AI095985, AI096040, AI102660, AI102691, OD011170, and HHSN261200800001E), the Bill and Melinda Gates Foundation (OPP1032817), and the Ragon Institute of MGH, MIT, and Harvard.

SUPPLEMENTARY MATERIALS

www.sciencemag.org/content/349/6245/320/suppl/DC1
Materials and Methods
Figs. S1 to S15
References

20 April 2015; accepted 17 June 2015
Published online 2 July 2015;
10.1126/science.aab3886

CIRCADIAN RHYTHMS

A protein fold switch joins the circadian oscillator to clock output in cyanobacteria

Yong-Gang Chang,[1] Susan E. Cohen,[2] Connie Phong,[3] William K. Myers,[4] Yong-Ick Kim,[2] Roger Tseng,[1,5] Jenny Lin,[3] Li Zhang,[1] Joseph S. Boyd,[2] Yvonne Lee,[6] Shannon Kang,[6] David Lee,[7] Sheng Li,[7] R. David Britt,[4] Michael J. Rust,[3] Susan S. Golden,[2,6] Andy LiWang[1,2,5,8,9]*

Organisms are adapted to the relentless cycles of day and night, because they evolved timekeeping systems called circadian clocks, which regulate biological activities with ~24-hour rhythms. The clock of cyanobacteria is driven by a three-protein oscillator composed of KaiA, KaiB, and KaiC, which together generate a circadian rhythm of KaiC phosphorylation. We show that KaiB flips between two distinct three-dimensional folds, and its rare transition to an active state provides a time delay that is required to match the timing of the oscillator to that of Earth's rotation. Once KaiB switches folds, it binds phosphorylated KaiC and captures KaiA, which initiates a phase transition of the circadian cycle, and it regulates components of the clock-output pathway, which provides the link that joins the timekeeping and signaling functions of the oscillator.

Endogenous circadian (~24-hour) rhythms are found in diverse organisms, arising as an adaptation to Earth's persistent cycles of night and day (*1*). To uncover the molecular mechanism of a circadian clock, we chose the cyanobacterial system because its oscillator can be reconstituted in vitro (*2*). The oscillator is composed of only three proteins KaiA, KaiB, and KaiC (*3*), which together generate a circadian rhythm of KaiC phosphorylation at residues serine 431 (S431) and threonine 432 (T432) in the CII domain (*4*, *5*). KaiA promotes KaiC (auto)phosphorylation during the subjective day (*4*, *6*), whereas KaiB provides negative feedback to inhibit KaiA (*7*, *8*) and promotes KaiC (auto)dephosphorylation during the subjective night. KaiB is also involved in regulating two antagonistic clock-output proteins—SasA (*9*) and CikA (*10*), which reciprocally control the master regulator of transcription, RpaA (*11*).

To determine the structure of KaiB in its KaiC-bound state, we used a monomeric variant of the KaiB-binding domain of KaiC, CI*, and a dimeric KaiB variant (*12*), KaiB*, with enhanced KaiC binding. Dimeric forms of free KaiB retain the same tertiary structure in crystals as tetrameric forms (*13*). Free KaiB has been shown by x-ray crystallography (*14*) to adopt a fold found in no other protein (*15*), despite clear sequence similarity with the thioredoxin-like fold at the N terminus of SasA, N-SasA (*9*). For structural studies, we used proteins from *Thermosynechococcus elongatus* (denoted by ^{te}), because they are more stable than those from *Synechococcus elongatus* (*16*). For functional studies, we used proteins from *S. elongatus* (denoted by ^{se}), the standard model for investigating in vivo

[1]School of Natural Sciences, University of California, Merced, CA 95343, USA. [2]Center for Circadian Biology, University of California, San Diego, La Jolla, CA 92093, USA. [3]Department of Molecular Genetics and Cell Biology, University of Chicago, Chicago, IL 60637, USA. [4]Department of Chemistry, University of California, Davis, CA 95616, USA. [5]Quantitative and Systems Biology, University of California, Merced, CA 95343, USA. [6]Division of Biological Sciences, University of California, San Diego, La Jolla, CA 92093, USA. [7]Department of Medicine, University of California, San Diego, La Jolla, CA 92093, USA. [8]Chemistry and Chemical Biology, University of California, Merced, CA 95343, USA. [9]Health Sciences Research Institute, University of California, Merced, CA 95343, USA.
***Corresponding author. E-mail: aliwang@ucmerced.edu**

Protective efficacy of adenovirus/protein vaccines against SIV challenges in rhesus monkeys

Dan H. Barouch *et al.*

Science **349**, 320 (2015);
DOI: 10.1126/science.aab3886